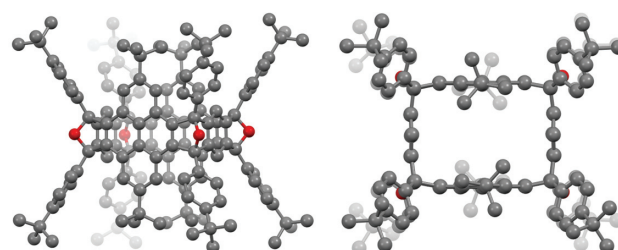# Synthesis of a Tetraepoxy Nanobelt and Its Reductive Aromatization Attempts

Yi Han[a]

Shaoqiang Dong[a]

Yuan Cheng Liau[a]

Chunyan Chi*[a]

[a] Department of Chemistry, National University of Singapore, 3 Science Drive 3, 117543, Singapore
chmcc@nus.edu.sg

✓ Facile synthesis of a tetraepoxy nanobelt with bulky substituents
✓ Tetrahydrogenated tetrabenzo[10]cyclacene was formed by reductive aromatization reaction with $TiCl_4/LiAlH_4$

Abstract Hydrocarbon nanobelts have recently attracted tremendous interest. Herein, we report our recent progress towards the synthesis of a newly designed hydrocarbon nanobelt tetrabenzo[10]cyclacene, which can be regarded as a sidewall fragment of the (10,0) carbon nanotube. The structures of both key intermediates — "U"-shape diepoxy building block and tetraepoxy nanobelt — were confirmed by single-crystal X-ray diffraction. Our preliminary reductive aromatization reactions revealed that a tetrahydrogenated species instead of tetrabenzo[10]cyclacene was formed during this process. Computational results further revealed that hydrogenation can lead to significant strain release of the backbone structure of tetrabenzo[10]cyclacene, which may attribute to the absence of the target compound during the reductive aromatization.

Key words hydrocarbon nanobelts, reductive aromatization, hydrogenation, strain

Introduction

Single-walled carbon nanotubes (SWCNTs) have attracted tremendous interest from scientists since they have intriguing physical properties[1] and wide applications, such as flexible electronics and energy storage.[2] However, current preparation methods of SWCNTs have limited capability to guarantee their exact structural uniformity. Successful atomically precise synthesis of SWCNTs is still restricted. Hydrocarbon nanobelts can be regarded as sidewall segments of SWCNTs. They can also serve as precursors for template synthesis of structurally uniform SWCNTs with defined carbon architectures and diameters.[3] They can be also used as model compounds to understand the fundamental properties of SWCNTs with different carbon architectures.[4] Just like SWCNTs, architectures of hydrocarbon nanobelts can also be categorized into armchair, zigzag, and chiral nanobelts (Figure 1a) with regard to the chiral indices of the corresponding SWCNTs (n, m).[5]

With the development of chemistry toolbox and iterative efforts of synthetic chemists, the first armchair and chiral hydrocarbon nanobelts have been synthesized by Itami's[6] and Miao's groups,[7] respectively, in recent years (Figure 1b). However, the attempted syntheses of the zigzag hydrocarbon nanobelts have only met partial success. Pioneer synthesis of zigzag carbon nanobelts led by Stoddart,[8] Cory,[9] and Schlüter[10] took advantage of repetitive Diels–Alder reactions on bisdiene and bisdienophile. Although the macrocyclic
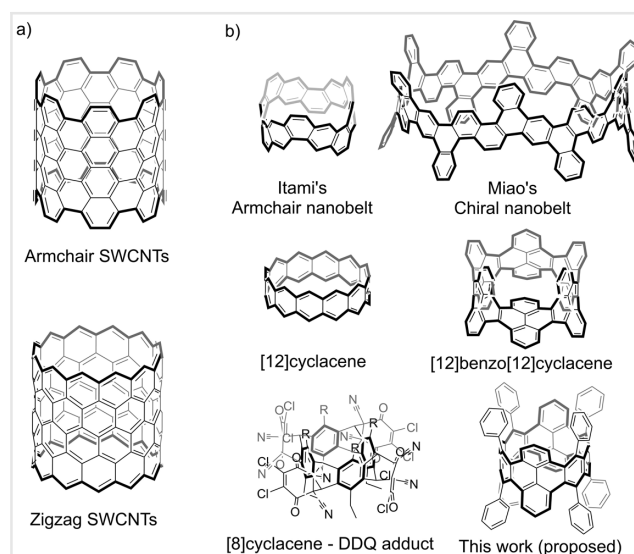

Figure 1 Representative structures of a) SWCNTs and b) recent progress towards hydrocarbon nanobelts.

precursors were obtained successfully, the final aromatization step could not be fully accomplished due to the increasing intrinsic strain during the reaction process. More recently, Peña's group took advantage of the Diels–Alder reaction between benzynes and furans and tried to perform deoxygenative aromatization on surface to synthesize [8] and [10] cyclacenes. However, only partial deoxygenation was achieved.[11] Wang's group recently tried to synthesize [8] cyclacene from resorcin[4]arenes, and so far only its adduct with four DDQs was fully characterized (Figure 1b).[12]

The extremely challenging synthesis of [n]cyclacenes originates from their high strain and poor stability. The closed-shell resonance form of [n]cyclacene contains only a diene-type conjugation without any aromatic sextet ring.[13] According to Clar's rule, such structure is predicted to be unstable. Furthermore, computational studies revealed that [n]cyclacene has an open-shell singlet ground state, which further demonstrates its high reactivity.[14] Annulation of benzene rings on the zigzag edge of [n]cyclacene is supposed to stabilize the whole structure.[15] In 2016, Itami's group proposed the synthesis of [n]benzo[n]cyclacenes (Figure 1b). However, rearrangement occurred at the final step and the target structure was not obtained.[15] Recently, Miao's group proposed the synthetic routes towards N-doped zigzag carbon nanobelt and tetrabenzo[10]cyclacene.[16] Although the precursors were successfully obtained and characterized, the hydrogenated molecules instead of target structures were formed in the last step. Another recent work on carbon nanobelts with partial zigzag edges was reported as a preprint by Itami and co-workers.[17]
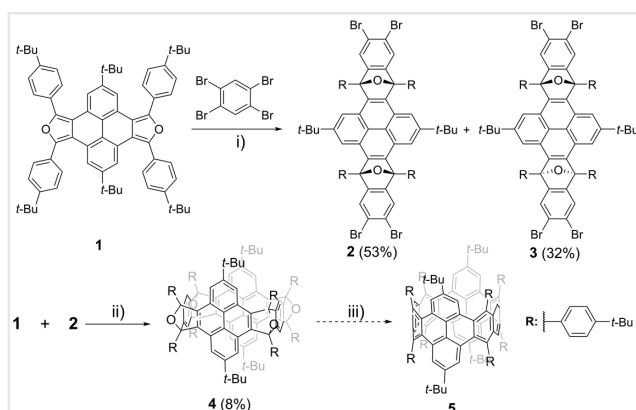
According to our experience towards the synthesis of long acenes, we believe that both benzo-annulation and attachment of kinetic protecting groups are the key strategies to stabilize cyclacene-like structures. We found that pyreno

[4,5-c:9,10-c']difuran reported by Mastalerz's and Zhang's groups[18] can serve as a good building block for the synthesis of hydrocarbon nanobelts for the following reasons. First, it can provide benzo-annulated cyclacene backbones which would introduce more Clar's sextets as compared to parent cyclacenes. Second, it can provide extra kinetic protections by attaching bulky groups. The solubility of this building block and the final compound will be improved as well. To push forward the limit of synthetic hydrocarbon nanobelts from the aspects of both strain and stability,[19] the synthetic route towards tetrabenzo[10]cyclacene was thus designed as shown in Scheme 1. Herein, we report the synthesis of the crucial intermediate—the tetraepoxy hydrocarbon cage **4**—and preliminary deoxygenation results, as well as strain analysis towards tetrabenzo[10]cyclacene **5**.

Results and Discussion

The synthetic route of tetraepoxy nanobelt **4** and tetrabenzo[10]cyclacene **5** is shown in Scheme **1**. Synthesis of the key precursor **1** is generally followed Mastalerz's report[18a] with an improved procedure. Compound **1** exhibits moderate stability in silica gel column but poor solubility in dichloromethane (DCM) and hexane, which makes purification difficult by column chromatography. Luckily, compound **1** could be purified by washing with ether. Benzyne was generated from 1,2,4,5-tetrabromobenzene in situ through a lithium–halogen exchange reaction and an elimination reaction at −15 °C in toluene.[20] Compound **1** then reacts with benzyne overnight to give the *cis*-isomer **2** and the *trans*-isomer **3** with 53% and 32% yield, respectively.[21] The structure of the *cis*-isomer **2** was confirmed by single-crystal X-ray diffraction (XRD).[22] It showed larger polarity than the *trans*-isomer **3** on TLC. Dibenzyne was then generated from the *cis*-isomer **2** and reacted with compound **1** to form the tetraepoxy nanobelt **4** with 8% yield.[23] The structure of **4** was also confirmed by single-crystal XRD.[24] Reductive deoxygenation of **4** was attempted by using various conditions, which will be discussed later.

Single crystals of **2** suitable for X-ray analysis were obtained by vapor diffusion of methanol into its chloroform solution. The crystal structure of **2** is shown in Figure 2 (a, b). Due to the oxygen bridge, the backbone of **2** has a "U"-shaped conformation. The dihedral angle θ between the terminal dibrominated phenyl rings and the central pyrene unit is 87°, which is smaller than that of disubstituted 9,10-epoxyanthracene counterpart.[25] Such a dihedral angle indicates that the formation of **4**, instead of other nanobelts with larger size, was favored. Bond angles α and β of the sp^3 carbon are 102° and 121°, respectively [Figure S4 in the Supporting Information (SI)]. The β angle is largely deviated from the normal sp^3 bond angle 109° due to steric hindrance between the substituted *tert*-butyl phenyl rings and the central *tert*-butyl pyrene unit.

Scheme 1 Synthetic route towards tetraepoxy nanobelt **4** and tetrabenzo[10]cyclacene **5**. (i) *n*-BuLi, −15 °C → rt, toluene, 1,2,4,5-tetrabromobenzene, overnight; (ii) *n*-BuLi, −15 °C → rt, toluene, overnight; (iii) reductive deoxygenation (various conditions were attempted, and are shown in Table 1).
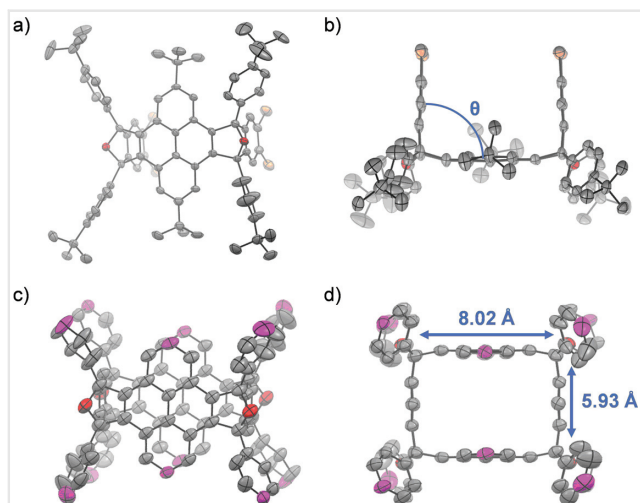
Figure 2 Single crystal structures of **2** (a: side view, b: top view) and **4** (c: side view, d: top view) drawn as ellipsoids set at 50% probability. Hydrogen atoms are all omitted for clarity. The *t*-butyl groups of **4** are omitted for clarity and the attached sites are highlighted in pink.

Figure 3 (a, b) Packing structure of **4** shown in space filling mode, hydrogens and *t*-butyl groups are omitted for clarity.

Figure 4 (a) Cyclic voltammograms and differential pulse voltammetry of **4** in DCM with Bu_4NPF_6 as the electrolyte; scanning rate is 0.1 V/s. (b) UV-vis absorption and fluorescence spectra of **4** in DCM.

Single crystals of **4** suitable for X-ray analysis were obtained by vapor diffusion of methanol into its THF solution. The crystal structure of **4** is shown in Figure 2 (c, d). The backbone of tetraepoxy nanobelt **4** is shaped like a small box, which is 8.02 Å long and 5.93 Å wide. The cavity of this box, however, may be too small to host some guest molecules for supramolecular chemistry studies. The packing of **4** was very loose due to the cyclic geometry as shown in Figure 3. No π–π interactions were observed between the neighboring molecules of **4**.

The electrochemical and optoelectronic properties of compound **4** were subsequently characterized and are shown in Figure 4. The cyclic voltammogram of **4** in DCM showed two reversible oxidation waves with a half-wave potential ($E_{1/2}^{ox}$) at 0.71 and 1.06 V, respectively (vs. Fc^+/Fc) (Figure 4a). However, no reduction wave was observed in the testing window. In DCM, compound **4** has a long-wavelength absorption maximum at 407 nm (Figure 4b). This absorption band is attributed to the S_0–S_1 transition as revealed by TD-DFT calculations (oscillator strength $f = 0.1308$). The band gap estimated from onset of low-energy edge of the absorption spectrum is 2.93 eV, which is in accordance with the computational result 3.13 eV (see also Figure S2 in SI). Compound **4** emits blue fluorescence with an emission maximum at 420 nm. The absolute external fluorescence quantum yield was measured to be 8.99% by using an integrating sphere.

Inspired by the successful synthesis of tetraepoxy nanobelt **4**, we proceeded to do the final step of reductive aromatization, which is not a trivial reaction.[26] Several conditions were examined as shown in Table 1. We first tr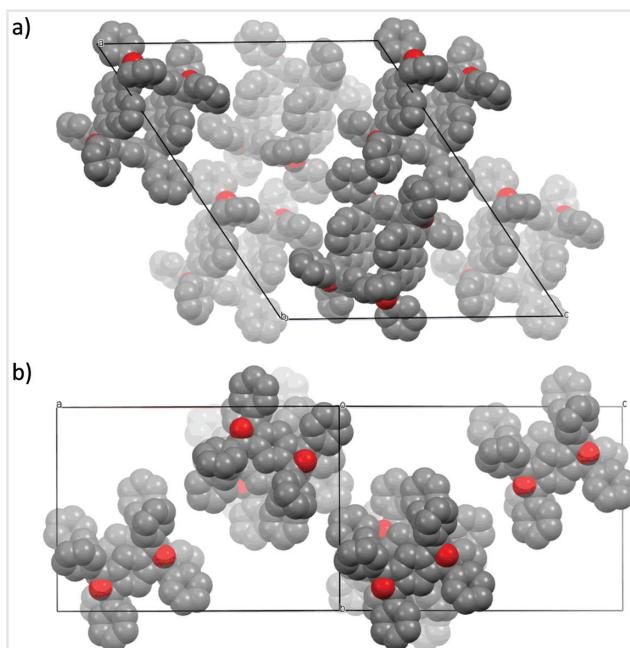ied reaction conditions 1 and 2 which are often used for the preparation of acenes.[27] However, the reaction did not take place since no new spot was observed on TLC and **4** remained unchanged. To avoid harsh conditions, we then tried reaction conditions 3 and 4.[28] Although deoxygenation

Organic Materials   Y. Han et al.   **Short Communication**

Table 1 Examined reductive aromatization conditions towards **5**

No.	Reaction conditions	Products detected by MALDI-TOF MS[a]
1	Zn, 10% AcOH in toluene, reflux	No reaction
2	TiCl$_4$, Zn, toluene, reflux	No reaction
3	TFA, Et$_3$SiH, CHCl$_3$, rt	Various hydrogenated products
4	TFA, 1,4-cyclohexadiene, CHCl$_3$, rt	Various hydrogenated products
5	TiCl$_3$·AlCl$_3$/n-BuLi, THF, 0 °C to rt	[**4** − O] and [**4** − 2 O]
6	TiCl$_4$/LAH 9:5, Et$_3$N, THF, reflux	[**4** − O] and [**4** − 2 O]
7	TiCl$_4$/LAH 3:8, Et$_3$N, THF, reflux	[**4** − 3 O]
8	TiCl$_4$/LAH 3:16, Et$_3$N, THF, reflux	[**5** + 4 H]

[a]Please refer to the Supporting Information (Figures S16–S19) for detailed mass spectra.

occurred, various hydrogenated products were observed, which was probably due to side reactions of deoxygenated intermediates with protonic acid. Condition 5 was subsequently attempted, which was proved to be effective for the reduction towards another strained system—twistacenes.[29] However, the deoxygenation was not complete for our system, even with a large excess amount of reductants. At the edge of surrender, we turned to the classical combination of TiCl$_4$/LiAlH$_4$ (LAH), which is widely applied in the reduction of unstrained endoxides as well as Mcmurry couplings.[30] Unexpectedly, we found that deoxygenation's progress could be promoted by decreasing the ratio of TiCl$_4$/LAH as seen under conditions 6–8. Although the final compound **5** was not observed on the MALDI-TOF mass spectrum, its tetrahydrogenated compound **6** was observed (Figure 5c). However, the low yield of the final step and purification issues hindered further characterization of compound **6**.

The absence of target compound **5** upon reductive aromatization can be attributed to its high intrinsic strain. The electronic structure of the backbone of **5** was calculated [B3LYP/6-31G(d,p)], which exhibits a close-shell ground state with a large band gap. Such electronic properties indicate that the backbone of **5** should be much more stable than the [10]cyclacene counterpart. Meanwhile, the strain of [10]cyclacene calculated from a hypothetical homodesmotic reaction was estimated to be 132 kcal/mol according to a previous report.[31] The strain of the backbone of **5**, as shown in Figure 6a, was estimated to be 136 kcal/mol, which is similar to that of [10]cyclacene. Such strain is much larger than that of any reported hydrocarbon nanobelt. We then calculated the intrinsic strain of dihydrogenated and tetrahydrogenated compounds of **5**, which are shown in Figure 6 (b, c). It revealed that dihydrogenation of **5** would release 43 kcal/mol of the intrinsic strain, so the strain of the dihydrogenated compound is about 93 kcal/mol. The strain of the tetrahydrogenated species was calculated to be 43 kcal/mol, which is 50 kcal/mol less than that of the dihydrogenated species. Such a strain release process
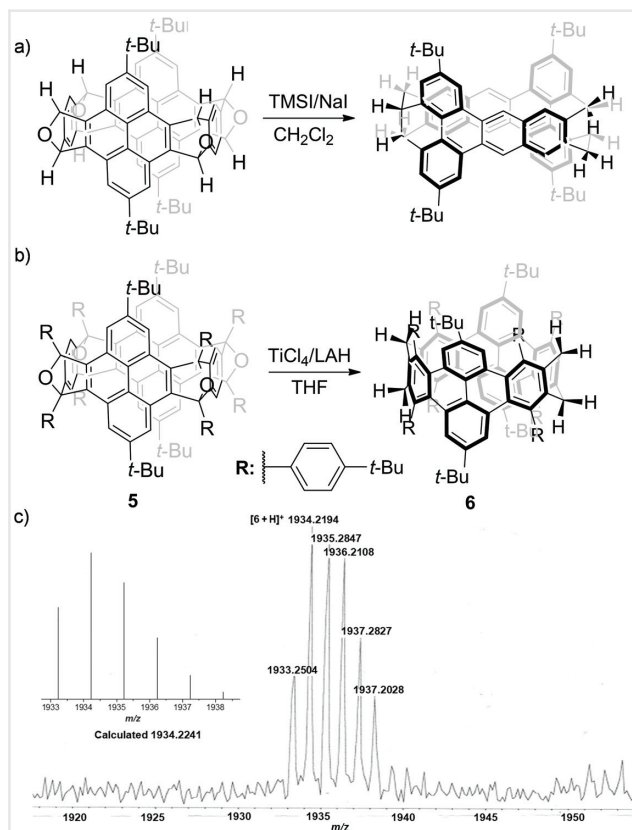

Figure 5 Different reductive products during attempts towards the synthesis of tetrabenzo[10]cyclacene, (a) Miao's report[16b] and (b) possible reaction and structure of **6** in this work, aromatic sextet rings are highlighted in bold. (c) High-resolution MALDI-TOF mass spectrum of **6**.
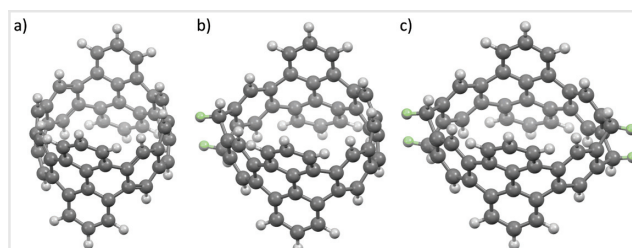

Figure 6 Molecular geometries optimized by DFT calculations (a) proposed nanobelt **5** without substituted phenyl groups, (b) dihydrogenated form of **5**, (c) compound **6** without substituted phenyl groups. The added hydrogens are highlighted with light green.

indicates that hydrogenation may happen easily during the reductive aromatization process and possibly explains the absence of compound **5** as the final product.

Interestingly, we noticed that our attempts at reductive aromatization reactions gave the product that differs from that in Miao's report.[16b] As shown in Figure 5a, a total of eight hydrogens were added to the backbone of tetrabenzo[10]cyclacene in Miao's work. The result was explained by the instability of the belt compound during

334

Organic Materials   Y. Han et al.   THIEME OPEN ACCESS   **Short Communication**

reductive aromatization due to the accumulating strain. However, in our case, only tetrahydrogenated compound **6** was observed in the MALDI-TOF mass spectrum (Figure 5c). As shown in Figure 5b, tetrahydrogenation most likely happened in the central benzene units since they are unprotected and are considered to be the most reactive sites according to Clar's rule. Our results indicate that attachment of proper protective groups along the backbone and reduction by the combination of $TiCl_4$/LAH may be promising strategies in the construction of hydrocarbon nanobelts with partial zigzag edges.

Conclusions

In summary, we reported our recent progress towards the synthesis of sidewall fragments of the (10,0) carbon nanotube. The structures of the precursor **2** and tetraepoxy belt **4** were unambiguously confirmed by single-crystal XRD. The preliminary results on reductive aromatization reactions revealed that $TiCl_4$/LAH in a lower ratio may be promising reductants for aromatization of epoxy-containing molecules with high strain. The tetrahydrogenated compound **6** was observed in the MALDI TOF mass spectrum during the reduction process. Our computational results revealed that the backbone of tetrabenzo[10]cyclacene is highly strained and hydrogenation can greatly release its strain. Thus, hydrogenation may happen easily during the reductive aromatization process and lead to the absence of **5** as the final product. Our results indicate that the combination of proper protective groups and reduction by $TiCl_4$/LAH may be the promising strategies in the construction of strained hydrocarbon nanobelts. We hope our results can provide valuable information towards the rational design and synthesis of hydrocarbon nanobelts with partial zigzag edges.

Funding Information

Acknowledgment

Supporting Information

Supporting Information for this article is available online at http://doi.org/10.1055/s-0040-1721101.

References And Notes

(1) (a) Tasis, D.; Tagmatarchis, N.; Bianco, A.; Prato, M. *Chem. Rev.* **2006**, *106*, 1105. (b) Dai, H. *Acc. Chem. Res.* **2002**, *35*, 1035. (c) Fennimore, A. M.; Yuzvinsky, T. D.; Han, W. Q.; Fuhrer, M. S.; Cumings, J.; Zettl, A. *Nature* **2003**, *424*, 408. (d) Cumings, J.; Zettl, A. *Science* **2000**, *289*, 602.

(2) (a) Yang, Z.; Ren, J.; Zhang, Z.; Chen, X.; Guan, G.; Qiu, L.; Zhang, Y.; Peng, H. *Chem. Rev.* **2015**, *115*, 5159. (b) Sun, H.; Zhang, Y.; Zhang, J.; Sun, X.; Peng, H. *Nat. Rev. Mater.* **2017**, *2*, 1.

(3) (a) Omachi, H.; Nakayama, T.; Takahashi, E.; Segawa, Y.; Itami, K. *Nat. Chem.* **2013**, *5*, 572. (b) Sanchez-Valencia, J. R.; Dienel, T.; Gröning, O.; Shorubalko, I.; Mueller, A.; Jansen, M.; Amsharov, K.; Ruffieux, P.; Fasel, R. *Nature* **2014**, *512*, 61.

(4) (a) Nishiuchi, T.; Feng, X.; Enkelmann, V.; Wagner, M.; Müllen, K. *Chem. Eur. J.* **2012**, *18*, 16621. (b) Quernheim, M.; Golling, F. E.; Zhang, W.; Wagner, M.; Räder, H. J.; Nishiuchi, T.; Müllen, K. *Angew. Chem. Int. Ed.* **2015**, *54*, 10341. (c) Lu, D.; Zhuang, G.; Wu, H.; Wang, S.; Yang, S.; Du, P. *Angew. Chem. Int. Ed.* **2017**, *56*, 158. (d) Huang, Q.; Zhuang, G.; Zhang, M.; Wang, J.; Wang, S.; Wu, Y.; Yang, S.; Du, P. *J. Am. Chem. Soc.* **2019**, *141*, 18938. (e) Hitosugi, S.; Nakanishi, W.; Yamasaki, T.; Isobe, H. *Nat. Commun.* **2011**, *2*, 492. (f) Sun, Z.; Ikemoto, K.; Fukunaga, T. M.; Koretsune, T.; Arita, R.; Sato, S.; Isobe, H. *Science* **2019**, *363*, 151. (g) Sisto, T. J.; Zakharov, L. N.; White, B. M.; Jasti, R. *Chem. Sci.* **2016**, *7*, 3681.

(5) Saito, R.; Fujita, M.; Dresselhaus, G.; Dresselhaus, M. S. *Appl. Phys. Lett.* **1992**, *60*, 2204.

(6) (a) Povie, G.; Segawa, Y.; Nishihara, T.; Miyauchi, Y.; Itami, K. *Science* **2017**, *356*, 172. (b) Povie, G.; Segawa, Y.; Nishihara, T.; Miyauchi, Y.; Itami, K. *J. Am. Chem. Soc.* **2018**, *140*, 10054.

(7) Cheung, K. Y.; Gui, S.; Deng, C.; Liang, H.; Xia, Z.; Liu, Z.; Chi, L.; Miao, Q. *Chem* **2019**, *5*, 838.

(8) (a) Kohnke, F. H.; Slawin, A. M. Z.; Stoddart, J. F.; Williams, D. J. *Angew. Chem. Int. Ed. Engl.* **1987**, *26*, 892. (b) Aston, P. R.; Isaacs, N. S.; Kohnke, F. H.; Slawin, A. M. Z.; Spencer, C. M.; Stoddart, J. F.; Williams, D. J. *Angew. Chem. Int. Ed. Engl.* **1988**, *27*, 966.

(9) (a) Cory, R. M.; Mcphail, C. L.; Dikmans, A. J.; Vittal, J. J. *Tetrahedron Lett.* **1996**, *37*, 1983. (b) Cory, R. M.; Mcphail, C. L. *Tetrahedron Lett.* **1996**, *37*, 1987.

(10) (a) Neudorff, W. D.; Lentz, D.; Anibarro, M.; Schlüter, A. D. *Chem. Eur. J.* **2003**, *9*, 2745. (b) Stuparu, M.; Lentz, D.; Rüegger, H.; Schlüter, A. D. *Eur. J. Org. Chem.* **2007**, *2007*, 88.

(11) Schulz, F.; García, F.; Kaiser, K.; Pérez, D.; Guitián, E.; Gross, L.; Peña, D. *Angew. Chem. Int. Ed.* **2019**, *58*, 9038.

(12) (a) Shi, T. H.; Guo, Q. H.; Tong, S.; Wang, M. X. *J. Am. Chem. Soc.* **2020**, *142*, 4576. (b) Wang, M.; Shi, T.; Tong, S. *Angew. Chem. Int. Ed.* **2020**. Doi: 10.1002/anie.202002827. (c) Zhang, Q.; Zhang, Y. E.; Tong, S.; Wang, M. X. *J. Am. Chem. Soc.* **2020**, *142*, 1196.

(13) Clar, E. The Aromatic Sextet. J. Wiley: London, **1972**.

(14) (a) Choi, H. S.; Kim, K. S. *Angew. Chem. Int. Ed.* **1999**, *38*, 2256. (b) Chen, Z.; Jiang, D. E.; Lu, X.; Bettinger, H. F.; Dai, S.; Schleyer, Pv.; Houk, K. N. *Org. Lett.* **2007**, *9*, 5449.

(15) Matsui, K.; Fushimi, M.; Segawa, Y.; Itami, K. *Org. Lett.* **2016**, *18*, 5352.

(16) (a) Wang, J.; Miao, Q. *Org. Lett.* **2019**, *21*, 10120. (b) Chen, H.; Gui, S.; Zhang, Y.; Liu, Z.; Miao, Q. *CCS Chem.* **2020**, *2*, 613.

(17) Cheung, K. Y.; Watanabe, K.; Segawa, Y.; Itami, K. *ChemRxiv* **2020**. Doi: 10.26434/chemrxiv.12324353.v2.

(18) (a) Baumgärtner, K.; Kirschbaum, T.; Krutzek, F.; Dreuw, A.; Rominger, F.; Mastalerz, M. *Chem. Eur. J.* **2017**, *23*, 17817. (b) Chen, W.; Long, G.; Kanehira, K.; Zhang, M.; Michinobu, T.; Liu, M.; Zhang, Q. *Asian J. Org. Chem.* **2018**, *7*, 2213.

(19) (a) Eisenberg, D.; Shenhar, R.; Rabinovitz, M. *Chem. Soc. Rev.* **2010**, *39*, 2879. (b) Segawa, Y.; Yagi, A.; Matsui, K.; Itami, K. *Angew. Chem. Int. Ed.* **2016**, *55*, 5136. (c) Lu, X.; Wu, J. *Chem* **2017**, *2*, 619. (d) Majewski, M. A.; Stępień, M. *Angew. Chem. Int. Ed.* **2018**, *58*, 86.

(20) (a) Haneda, H.; Eda, S.; Aratani, M.; Hamura, T. *Org. Lett.* **2014**, *16*, 286. (b) Eda, S.; Hamura, T. *Molecules* **2015**, *20*, 19449.

(21) **Synthetic procedure for compounds 2 and 3**: Compound **1** (923 mg, 1 mmol) and 1,2,4,5-tetrabromobenzene (7.8 g, 20 mmol) were dissolved in 400 mL anhydrous toluene and cooled to −15 °C. *n*-BuLi (2 M in hexane, 5 mL, 10 mmol) was added dropwise into the reaction mixture. The reaction mixture was then warmed up to room temperature overnight. Saturated NH_4Cl solution was used to quench the reaction. The solution was further washed with water and the organic layer was dried over Na_2SO_4. The residue was purified via column chromatography (silica, hexane:DCM, 1:1 v/v) to yield **2** (723 mg, 52%) and **3** (445 mg, 32%) as white solids. Compound **2**: [1] H NMR (400 MHz, chloroform-*d*): δ = 7.95 (d, *J* = 8.0 Hz, 8 H), 7.80 (s, 4 H), 7.73 (s, 4 H), 7.57 (d, *J* = 8.5 Hz, 8 H), 1.38 (s, 36 H), 0.99 (s, 18 H). [13] C NMR (126 MHz, chloroform-*d*): δ = 152.93, 152.74, 148.89, 147.93, 131.12, 129.85, 126.78, 126.35, 125.91, 122.58, 121.29, 119.39, 92.67, 35.05, 34.94, 31.40, 31.24. HRMS analysis (APCI) calcd. for $C_{80}H_{79}Br_4O_2$ $(M + H)^+$: 1387.2808; found: 1387.2803 (error: 0.4 ppm). Compound **3**: [1] H NMR (400 MHz, chloroform-*d*): δ = 7.92 (br, 12 H), 7.77 (s, 4 H), 7.55 (d, *J* = 8.4 Hz, 8 H), 1.36 (s, 36 H), 0.99 (s, 18 H). [13] C NMR (126 MHz, chloroform-*d*): δ = 152.94, 152.84, 148.56, 148.04, 131.47, 127.00, 125.94, 125.89, 122.45, 121.32, 119.53, 92.53, 35.09, 34.93, 31.39, 31.24. HRMS analysis (APCI) calculated for $C_{80}H_{79}Br_4O_2$ $(M + H)^+$: 1387.2808; found: 1387.2809 (error: −0.1 ppm).

(22) X-ray crystallographic data for compound **2** were deposited in the Cambridge Crystallographic Data Centre (CCDC) with the number of 2020884.

(23) **Synthetic procedure for compound 4**: Compound **1** (507 mg, 0.55 mmol) and **2** (850 mg, 0.61 mmol) were dissolved in anhydrous toluene (150 mL) under an inert atmosphere and cooled to −15 °C. *n*-BuLi (2 M in hexane, 1.5 mL 3 mmol) was added dropwise into the reaction mixture. The reaction mixture was then warmed up to room temperature overnight. Saturated NH_4Cl solution was used to quench the reaction. The residue was purified via column chromatography (silica, hexane:DCM, 1:1 v/v) to yield compound **4** (70 mg, 52%) as a white solid. [1] H NMR (400 MHz, chloroform-*d*): δ = 8.00 (br, 16 H), 7.59 (br, 20 H), 7.37 (s, 8 H), 1.39 (s, 72 H), 0.72 (s, 36 H). [13] C NMR (126 MHz, chloroform-*d*): δ = 152.37, 150.66, 149.45, 146.93, 132.58, 125.84, 125.67, 121.57, 118.02, 116.48, 93.27, 34.94, 34.63, 31.46, 31.21. HRMS analysis (APCI) calculated for $C_{148}H_{153}O_4$ $(M + H)^+$: 1994.1763; found: 1994.1768 (error: −0.2 ppm).

(24) X-ray crystallographic data for compound **4** were deposited in the Cambridge Crystallographic Data Centre (CCDC) with the number of 2020888.

(25) Miyamoto, N.; Nakazawa, Y.; Nakamura, T.; Okano, K.; Sato, S.; Sun, Z.; Isobe, H.; Tokuyama, H. *Synlett* **2018**, *29*, 513.

(26) Marshall, J. L.; Lehnherr, D.; Lindner, B. D.; Tykwinski, R. R. *ChemPlusChem* **2017**, *82*, 967.

(27) (a) Chun, D.; Cheng, Y.; Wudl, F. *Angew. Chem. Int. Ed.* **2008**, *47*, 8380. (b) Dai, G.; Chang, J.; Zhang, W.; Bai, S.; Huang, K. W.; Xu, J.; Chi, C. *Chem. Commun.* **2015**, *51*, 503.

(28) Tokuyama, H.; Miyamoto, N.; Nakazawa, Y.; Nakamura, T.; Okano, K.; Sato, S.; Sun, Z.; Isobe, H. *Synlett* **2017**, *29*, 513.

(29) (a) Lu, J.; Ho, D. M.; Vogelaar, N. J.; Kraml, C. M.; Pascal, R. A. Jr *J. Am. Chem. Soc.* **2004**, *126*, 11168. (b) Lu, J.; Ho, D. M.; Vogelaar, N. J.; Kraml, C. M.; Bernhard, S.; Byrne, N.; Kim, L. R.; Pascal, R. A. Jr *J. Am. Chem. Soc.* **2006**, *128*, 17043. (c) Xiao, Y.; Mague, J. T.; Schmehl, R. H.; Haque, F. M.; Pascal, R. A. *Angew. Chem. Int. Ed.* **2019**, *58*, 2831.

(30) (a) Mcmurry, J. E.; Fleming, M. P. *J. Org. Chem.* **1975**, *40*, 2555. (b) Mcmurry, J. E.; Silvestri, M. G.; Fleming, M. P.; Hoz, T.; Grayston, M. W. *J. Org. Chem.* **1978**, *43*, 3249. (c) Hart, H.; Nwokogu, G. *J. Org. Chem.* **1981**, *46*, 1251. (d) Wong, H. N. C. *Acc. Chem. Res.* **1989**, *22*, 145.

(31) (a) Segawa, Y.; Yagi, A.; Ito, H.; Itami, K. *Org. Lett.* **2016**, *18*, 1430. (b) Minkin, V. I. *Pure Appl. Chem.* **1999**, *71*, 1919. (c) George, P.; Trachtman, M.; Bock, C. W.; Brett, A. M. *Tetrahedron* **1976**, *32*, 317.